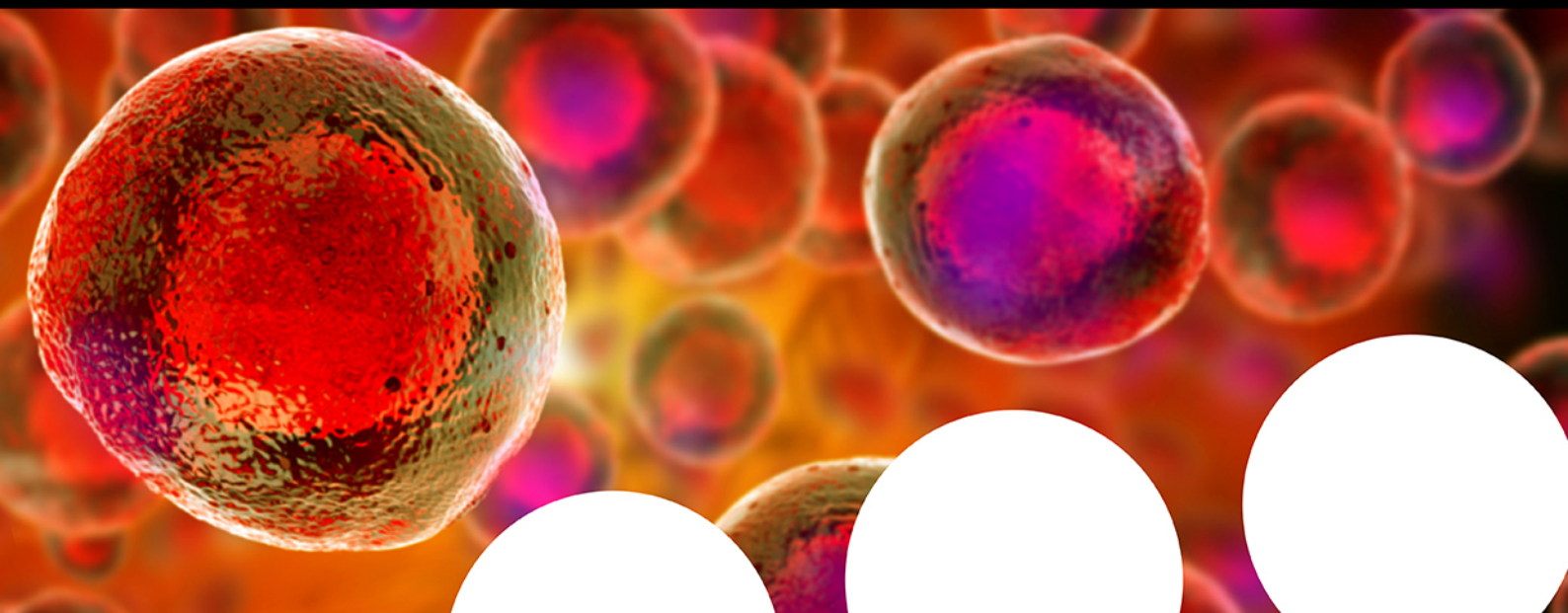


Your research is important and needs to be shared with the world



Benefit from the Chemistry Europe Open Access Advantage

- Articles published open access have higher readership
- Articles are cited more often than comparable subscription-based articles
- All articles freely available to read, download and share.

Submit your paper today.



www.chemistry-europe.org

6-Methylquinazolin-4(3H)-one Based Compounds as BRD9 Epigenetic Reader Binders: A Rational Combination of *in silico* Studies and Chemical Synthesis

Ester Colarusso,^[a] Erica Gazzillo,^[a, b] Eleonora Boccia,^[a, b] Assunta Giordano,^[a, c] Maria Giovanna Chini,^[d] Giuseppe Bifulco,^{*,[a]} and Gianluigi Lauro^{*,[a]}

Dedicated to Professor Cesare Gennari on the occasion of his 70th birthday

6-methylquinazolin-4(3H)-one-based compounds were here identified and synthesized as novel binders of bromodomain-containing protein 9 (BRD9) epigenetic reader. Accounting a fast and efficient synthetic route aimed to easily obtain differently 2- and 8-disubstituted 6-methylquinazolin-4(3H)-one derivatives, a virtual library of synthesizable items was built and submitted to molecular docking experiments. Based on two 3D structure-based pharmacophore models recently developed by us on BRD9, 16 compounds were selected and synthesized,

using mild conditions with good yields in relatively short reaction times. Among them, **14**, **16**, **18**, **22**, and **26** emerged as the most potent compounds of these series, able to bind BRD9 at the low micromolar range of concentrations. These molecules also showed a promising selective behavior when tested against BRD4 bromodomain. These results highlighted the quinazolin-4(3H)-one chemical core as a valuable scaffold for developing promising BRD9 binders.

Introduction

Bromodomains (BRDs) are protein domains that selectively recognize and bind ϵ -N-acetyl-lysine residues histone tails and play a key role in gene expression. Since the first discovery, bromodomains have been found in many nuclear proteins. In particular, the human genome encodes 61 BRDs in 46 different proteins with catalytic functions involved in some pathological processes and present in most tissues.^[1]

Bromodomain-containing proteins are grouped into eight main families. The BET family (Bromo- and Extra-Terminal-Domain), including BRD2, BRD3, BRD4, and BRDT proteins, is the most studied and it plays a central role in cell cycle progression, cellular proliferation, and apoptosis.^[2] As a subunit of the SWI/SNF chromatin remodeling complexes, non-BET bromodomain containing protein BRD9 has recently emerged as an interesting target due to its involvement in cancer.^[3] Specifically, it is part of BAF complexes (e.g., ncBAF and nBAF) and, as an epigenetic reader, it is involved in post-translational modifications.^[4] In pathological conditions, BRD9 overexpression has been detected and, accordingly, its involvement in tumors, including acute myeloid leukemia (AML), renal carcinoma, non-small cell lung cancer, malignant tumors, rhabdoid tumor, breast cancer, cervical carcinoma, and hepatocellular carcinoma has been reported.^[4]

Starting from these premises, the identification of a new class of BRD9 binders is required for further interrogating the biological role of this protein. In this paper, starting from the broad spectrum of biological and pharmacological activities^[5] already reported for quinazolin-4(3H)-one-based compounds, the 6-methylquinazolin-4(3H)-one scaffold was selected with the aim of developing novel compounds targeting BRD9. Coupling the efficiency/fastness of the chosen synthetic route and the high performance of BRD9 3D pharmacophore model^[6] recently developed by us in predicting promising compounds, a library of synthesizable items was built *in silico* and submitted to molecular docking-based virtual screening. After this step, 16 compounds were synthesized after selecting the more convenient strategy.^[7] Finally, *in vitro* bioscreen led to 5 compounds (**14**, **16**, **18**, **22**, and **26**) able to bind BRD9 in the low micromolar range of concentration by AlphaScreen assays. Since quinazolin-4(3H)-one-based compounds were also re-

[a] Dr. E. Colarusso, E. Gazzillo, E. Boccia, Dr. A. Giordano, Prof. G. Bifulco, Dr. G. Lauro
Department of Pharmacy, University of Salerno
Via Giovanni Paolo II 132, 84084 Fisciano (SA), Italy
E-mail: bifulco@unisa.it
glauro@unisa.it
https://computorgchem.unisa.it

[b] E. Gazzillo, E. Boccia
Ph.D. Program in Drug Discovery and Development
University of Salerno
Via Giovanni Paolo II 132, 84084 Fisciano (SA), Italy

[c] Dr. A. Giordano
Institute of Biomolecular Chemistry (ICB), Consiglio Nazionale delle Ricerche (CNR)
Via Campi Flegrei 34, 80078 Pozzuoli (NA), Italy

[d] Dr. M. G. Chini
Department of Biosciences and Territory, University of Molise
C.da Fonte Lappone- 86090, Pesche (IS), Italy

Supporting information for this article is available on the WWW under
https://doi.org/10.1002/ejoc.202200868

Part of the "Cesare Gennari's 70th Birthday" Special Collection.

© 2022 The Authors. European Journal of Organic Chemistry published by Wiley-VCH GmbH. This is an open access article under the terms of the Creative Commons Attribution Non-Commercial NoDerivs License, which permits use and distribution in any medium, provided the original work is properly cited, the use is non-commercial and no modifications or adaptations are made.

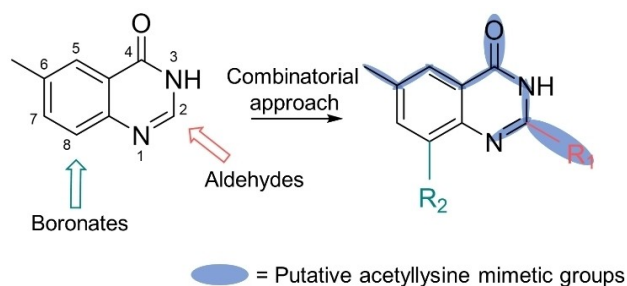
cently reported as BRD4 binders,^[8] the ability of the five newly identified molecules to target BRD4 was also investigated, obtaining a poor binding and highlighting their selective profile against BRD9.

Results and Discussion

The privileged scaffold feature of the quinazolin-4(3*H*)-one^[9] and the possibility of easily decorating it in different ways prompted us to investigate it as a starting point for developing BRD9 ligands.

With this aim, since all BRD9 binders feature an acetyl lysine mimetic group needed for the binding^[6,10], the inclusion of a hydrophobic group on this scaffold, e.g., a methyl, was here accounted in order to have *a priori* a function that could satisfy this condition (Scheme 1). Among the set of possible quinazolin-4(3*H*)-one functionalized derivatives, the 6-methylquinazolin-4(3*H*)-one was specifically selected for further investigations due to its compatibility with facile synthetic procedures (*vide infra*) and because preliminary *in silico* analysis disclosed its ability to reproduce a binding mode compatible with the requirements for BRD9 binding.

Indeed, we firstly performed computational studies by means of docking calculations and pharmacophore screening, in order to validate this chemical core as promising molecular platform for the development of new BRD9 binders.^[11] Prior to accurately developing a synthetic procedure leading to the building of a combinatorial library of 6-methylquinazolin-4(3*H*)-one derivatives, the selected core was docked onto the BRD9 binding site (PDB code: 5F1H).^[10a] Subsequently, the output docking poses were screened through 3D structure-based pharmacophore model, i.e., AHRR 4-points model ("pharm-fragment"), AAHRRRX 7-points model ("pharm-druglike1") and AAHRRRX 7 points model ("pharm-druglike2") developed by us and previously reported (Figure 1 and Figure S1). In this way, we firstly assessed whether the chosen core would feature minimum requirements to bind BRD9 (according to "pharm-fragment" model) and, secondly, the possible functionalization positions were identified on the selected poses in order to rationally design optimized derivatives (according to "pharm-druglike1" and "pharm-druglike2" models).^[6] The obtained results highlighted three possible binding modes, here named



Scheme 1. Rational design for 6-methylquinazolin-4(3*H*)-one chemical derivatives.

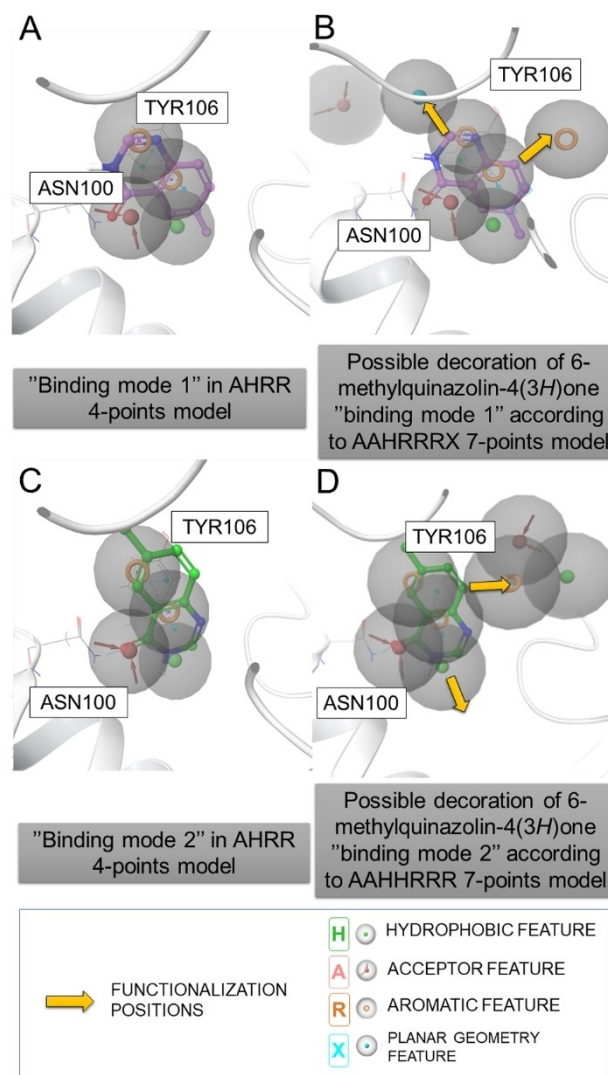


Figure 1. "Binding mode 1" of 6-methylquinazolin-4(3*H*)-one in A) "pharm-fragment" and B) "pharm-druglike2"; "Binding mode 2" of 6-methylquinazolin-4(3*H*)-one in C) "pharm-fragment" and D) "pharm-druglike1".

"binding mode 1", "binding mode 2", and "binding mode 3" (Figure 1A, Figure 1C and Figure S2C), in which three different portions of the chemical core covered the acetyl lysine mimic function specifically represented by the two of the four features of "pharm-fragment" model, namely "A" as H-bond acceptor group and "H" as a hydrophobic feature. Subsequently, the three selected poses of the 6-methylquinazolin-4(3*H*)-one scaffold were analyzed according to the "pharm-druglike2" and "pharm-druglike1" pharmacophore models (Figure 1 and Figure S2) to evaluate which of the models could be accounted for the subsequent design of optimized derivatives.

Regarding "binding mode 1", "pharm-druglike2" (AAHRRRX 7-points) model was selected since, in this way, the starting scaffold could be satisfactorily decorated in both positions 2 and 8 (Figure 1B, Scheme 1). Conversely, "pharm-druglike1" was only compatible for substitution at 8 position (Figure S2G). For "binding mode 2", "pharm-druglike1" model was chosen since

the starting core could be functionalized in 2 and 8 positions as well (Figure 1D).

It is worth noting that, in this case, position 2 corresponded to the "H" hydrophobic function belonging to the necessary acetyl lysine mimetic group and, accordingly, it could be functionalized with alkyl substituents, whereas position 8 could allow the decoration with aromatic ("R"), H-bond acceptor ("A") and hydrophobic ("H") substituents. On the other hand, "pharm-druglike2" was considered less suitable for the design of highly decorated derivatives due to the fact that the position of the 6-methyl substituent prevented the decoration towards the planar ("X") and the adjacent H-bond acceptor ("A") functions while only leaving a simple aromatic ("R") moiety for the optimization (Figure S2E). Regarding "binding mode 3", neither "pharm-druglike1" nor "pharm-druglike2" pharmacophore models were compatible for the subsequent decoration (Figure S2F and S2I), and it was discarded for orienting the synthesis of derivatives. Unless the only insertion of the hydrophobic group as acetyl lysine mimetic, putative further functionalizations aimed to explore the chemical space of the binding site would have required a chemical alteration of the starting scaffold (Figure S2F and S2I).

In light of these computational data, we then selected the faster and easier synthetic strategy (Scheme 2) to obtain 6-methylquinazolin-4(3H)-one derivatives, based on the use of aldehydes and aromatic boronic acids (at 2 and 8 positions, respectively). Accordingly, starting from commercially available items, a virtual library of ~175,000 compounds (See Experimental Section) was built and used as input for molecular docking calculation against BRD9. The output docking poses were then screened through 3D structure-based "pharm-druglike1" and "pharm-druglike2" pharmacophore models, and finally, 16 compounds featuring good docking scores (see Experimental Section), satisfactory matching of the pharmacophoric features, and promising PhaseScreen scores (see Experimental Section) (Table 1 and Table 2) were selected for the chemical synthesis phase.

Specifically, compounds 12–22 were selected with "pharm-druglike2" (AAHRRRX 7-points) pharmacophore model (Table 2). Also, compounds 23–24 were selected as negative controls (Table 2) to evaluate and corroborate the reliability of the 3D

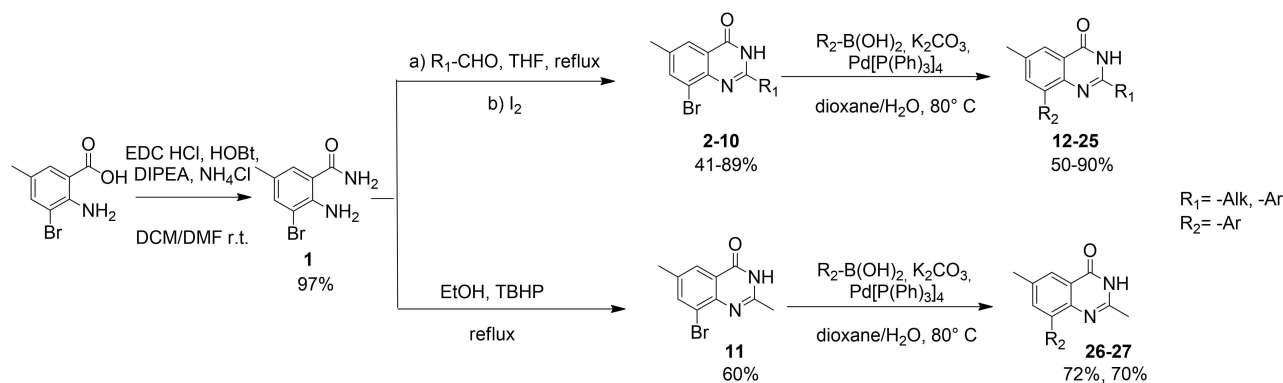
structure-based pharmacophore models, since they only meet five of the seven points of the pharmacophore model. In addition, three derivatives, 25–27 (Table 2), were selected through "pharm-druglike1" (AAHRRR 7-points) model.

Subsequently, after selecting the best molecules, we opted for a versatile synthetic strategy that would allow us to obtain the maximum chemical diversity in the shortest number of synthetic steps (Scheme 2).

Indeed, due to the high interest of medicinal chemistry^[9] for the quinazolin-4(3H)-one nucleus related to the multiple biological functions, many synthetic methods are already reported for these compounds. However, most methods involve prolonged reaction times, high catalyst loading and less suitable to optimization procedures.^[12] In light of this, we decided to build the quinazolin-4(3H)-one nucleus with a one-pot multistep procedure by a condensation reaction of the aminobenzamide 1 with the corresponding aldehydes followed by oxidative dehydrogenation catalyzed by I₂ (Scheme 2).^[7]

Starting from the 2-amino-3-bromo-5-methylbenzoic acid, the corresponding amide was generated with 97% of yield. In the next synthetic step, since the polar nature of the obtained derivative 1, instead of functionalizing position 8, we preferred to synthesize the quinazolin-4(3H)-one core with consequent more accessible purification procedures. Compound 1 reacted with the different aldehydes in THF at reflux with the formation of an imine in position 2,^[7] followed by intramolecular cyclization promoted by iodine addition, obtaining compounds 2–10 (see Table 1, yield: 41–89%). Due to the high volatility of the acetaldehyde, which is difficult to manage also at room temperature, the intermediate 11, bearing a methyl in position 2, was obtained by oxidizing ethanol with the TBHP, in order to obtain the acetaldehyde *in situ*.

Final compounds 12–27 were obtained with Suzuki-Miyaura cross-coupling, which allowed us to simply functionalize position 8 with the selected aromatic rings, leading to moderate-to-good yields (50–90%) under mild conditions. To prepare the designed compounds, the cross-coupling was performed under standard conditions using Pd[P(Ph)₃]₄ as the catalyst and aqueous carbonate base in a water/dioxane at 80 °C (Scheme 2).



Scheme 2. Synthetic strategy for compounds 12–27.

Table 1. Chemical structures of compounds 2–27.

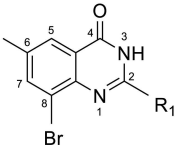
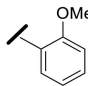
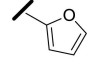
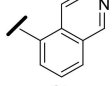
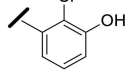
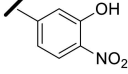
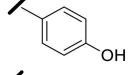
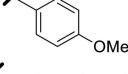
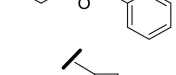
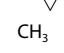
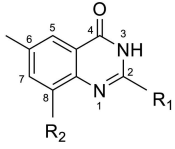
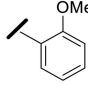
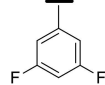
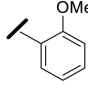
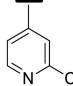
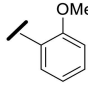
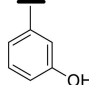
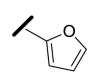
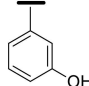
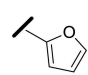
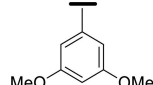
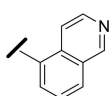
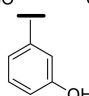
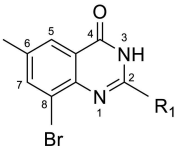
				
Compound	R ₁	Br	R ₂	Yield
2				97%
3				63%
4				44%
5				66%
6				89%
7				66%
8				75%
9				88%
10				56%
11	CH ₃			60%
				
Compound	R ₁	Br	R ₂	Yield
12				66%
13				78%
14				54%
15				55%
16				73%
17				62%

Table 1. continued



Compound	R ₁	R ₂	Yield
18			66%
19			72%
20			82%
21			90%
22			80%
23			50%
24			75%
25			61%
26	CH ₃		72%
27	CH ₃		70%

Table 2. *In silico* predicted parameters accounted for the selection of compounds 12–27.

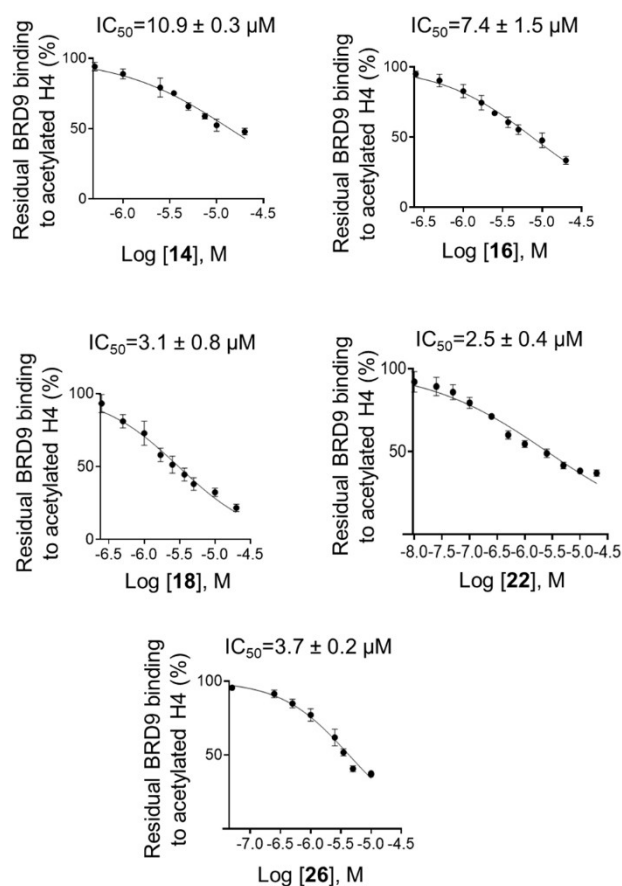
Compound	Docking score	Num sites matched	PhaseScreen score	Hypo ID
12	-8.3	6/7	1.61	AAHRRRX
13	-8.1	6/7	1.60	AAHRRRX
14	-7.8	6/7	1.61	AAHRRRX
15	-8.0	6/7	1.58	AAHRRRX
16	-8.8	6/7	1.55	AAHRRRX
17	-7.4	6/7	1.56	AAHRRRX
18	-7.8	6/7	1.67	AAHRRRX
19	-7.5	6/7	1.52	AAHRRRX
20	-7.5	6/7	1.57	AAHRRRX
21	-7.8	6/7	1.60	AAHRRRX
22	-7.8	6/7	1.59	AAHRRRX
23	-7.5	5/7	1.61	AAHRRRX
24	-6.9	5/7	1.18	AAHRRRX
25	-7.3	6/7	1.74	AAHRRRX
26	-9.2	6/7	1.52	AAHRRRX
27	-8.8	6/7	1.95	AAHRRRX

Table 3. Residual activity and IC₅₀ values of compounds 12–27 against BRD9 and BRD4. Data of the residual enzyme activity at 10 μM test compound concentration are given as means ± S.D. for n = 3.

Compound	Residual binding of Histone H4Ac to BRD9 (%) ± S.D.	IC ₅₀ ± S.D. for BRD9 (μM)	Residual binding of Histone H4Ac to BRD4 BD1 (%) ± S.D.
12	63.3 ± 1.6	/	/
13	69.5 ± 0.9	/	/
14	56.0 ± 1.2	10.9 ± 0.3	91.9 ± 1.4
15	71.1 ± 1.3	/	/
16	53.6 ± 2.4	7.4 ± 1.5	91.9 ± 1.5
17	64.3 ± 2.0	/	/
18	42.5 ± 0.3	3.1 ± 0.8	77.6 ± 1.6
19	76.3 ± 0.7	/	/
20	68.0 ± 3.2	/	/
21	65.6 ± 2.0	/	/
22	42.9 ± 2.1	2.5 ± 0.4	85.1 ± 1.6
23	77.8 ± 4.5	/	/
24	74.9 ± 2.2	/	/
25	66.1 ± 1.6	/	/
26	44.6 ± 0.3	3.7 ± 0.2	86.0 ± 1.0
27	76.6 ± 2.9	/	/

In order to determine the binding affinity of the synthesized derivatives 12–27, all the compounds were preliminarily screened by AlphaScreen assays,^[13] evaluating their potential affinity against BRD9 protein at 10 μM starting concentration. Interestingly, most of the synthesized compounds (11/16) led to a residual binding of histone H4Ac to BRD9 < 70% (Table 3). Among them, compounds 14, 16, 18, 22, and 26 showed the best binding affinity against the protein, with a percentage of acetylated histone residual binding between 42.5% and 56.0% (Table 3). The biological profile of these compounds was further investigated by calculating the corresponding IC₅₀ values, obtaining for them a promising affinity for the protein in the low micromolar range of affinities (Table 3 and Figure 2). Conversely, 15, 19, 23, 24, 27 did not exhibit a significant binding to BRD9, with residual binding of acetylated histone between 70% and 80% (Table 3).

Data arising from compounds 14, 16, 18, 22, and 26, selected by *in silico* investigations and featuring promising binding affinities, highlighted the reliability of the proposed workflow. Indeed, they respected 6/7 points of the 3D structure-based pharmacophore models and this guaranteed *a priori* that specific functional groups are in the binding site area while also establishing key interactions with the protein counterpart. After visual inspection, the interactions with the fundamental amino acids and 14, 16, 18, 22 and 26 were confirmed: the carbonyl group of the quinazolinone core (that matches the pharmacophore acceptor feature “A”) established an H-bond with Asn 100 (Figure 3), which is a key amino acid for the recognition of acetylated lysine residues.^[10c,14] In addition, aromatic rings matching the aromatic features (“R”) of the AAHRRRX and AAHHRRR models, derived from substituents introduced on the quinazolinone-based scaffold, were able to establish π-π interactions with Tyr 106 and Phe 44, representing key amino acids essential for BRD9 activity (Figure 3).^[10c,14] Moreover, structure-activity analysis indicated that, among the compounds selected through “pharm-druglike2” model (14, 16, 18, and 22, Figure 3A–3D), 16, 18, and 22, featuring a 3,5-dimethoxyphenyl substituent at position 8, showed the best binding behavior. Interestingly, mono- or di-methoxy substi-

**Figure 2.** Concentration-response curves for the analysis of the binding of compounds 14, 16, 18, 22, and 26 on BRD9. Data are expressed as a percentage related to that of control (100%), means with S.D., n = 3.

tuted phenyl moieties were also reported in several BRD9 binders already identified.^[10a-c] Among the set of compounds selected with “pharm-druglike1” model, 26 (Figure 3E) showed an encouraging activity as well, suggesting that the 6-methylquinazolin-4(3*H*)-one can be accommodated in the BRD9 binding site respecting two different predicted binding modes.

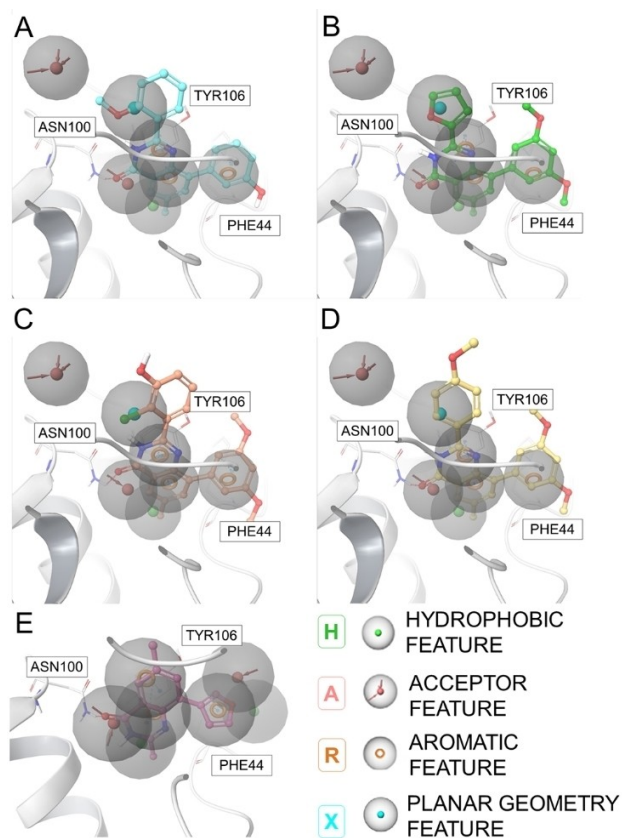


Figure 3. Superposition of **14** (colored by atom type: C cyan, O red, N blue, polar H light grey), **16** (colored by atom type: C green, O red, N blue, polar H light grey), **18** (colored by atom type: C light pink, O red, N blue, polar H light grey), and **22** (colored by atom type: C yellow, O red, N blue, polar H light grey) with “pharm-druglike2” model (panel A, B, C and D, respectively). Superposition of **26** (colored by atom type: C fuchsia, O red, N blue, polar H light grey) with “pharm-druglike1” model (panel E). All the compounds and 3D structure-based pharmacophore models are shown onto BRD9 binding site (PDB code: 5F1H, represented with grey ribbons). Key interactions (H-bond in red and π - π stacking in blue) with fundamental amino acids (Asn 100, Tyr 106 and Phe 44) and **14**, **16**, **18**, **22** and **26** are also shown.

Compounds **23** and **24**, selected as “negative controls” (matching 5/7 features of the “pharm-druglike2” pharmacophore model) did not show a promising binding, as expected.

Furthermore, in order to get more insights into the activity of quinazolinone-based derivatives on BRD9, molecular dynamics (MD) simulations (see Experimental section) for the most promising compound, i.e., **22**, and the least active one, i.e., **23**, were performed.^[14b] Firstly, the root mean square deviation (RMSD) values, computed for the ligands/protein backbone complex and for the ligand sampled conformations along the whole simulation vs. their starting reference coordinates, were evaluated in order to appraise the stability of the complexes. The RMSD analysis corroborated the experimental results, since **23** showed higher RMSD values if compared with those of **22**. Also, larger fluctuations were detected for **23**, highlighting the instability in maintaining protein binding (Figure S3). In addition, analysis of protein interactions along time showed that **22**, if compared with **23**, was able to establish and preserve interactions with key amino acids (Asn 100, Tyr 106 and Phe

44). Interestingly, for compound **22** we observed constant contacts along the simulations. Indeed, **22** was able to establish interaction with Asn 100 (interaction fraction value = 1.6) (Figure S3).

Considering that quinazolin-4(3H)-one derivatives were already reported as BET family member BRD4 binders,^[8] compounds **14**, **16**, **18**, **22**, and **26** were also evaluated on the first bromodomain of BRD4 (BRD4 BD1) by AlphaScreen assays. Interestingly, they did not exhibit significant binding against BRD4 BD1 (Table 3), thus emerging as novel BRD9 binders while also featuring a promising selective behavior.

Conclusion

In summary, 6-methylquinazolin-4(3H)-one-based compounds were here identified as novel BRD9 binders by coupling accurate *in silico* investigations and a fast and efficient chemical synthesis procedure. This workflow led to the careful selection of a set of promising items, which were quickly synthesized in moderate-to-good yields.

In particular, following an efficient synthetic procedure, involving three steps, the selected compounds were synthesized starting from 2-amino-3-bromo-6-methylbenzamide, obtained from the corresponding acid. Imine formation followed by the cyclization reactions gave the 6-methylquinazolin-4(3H)-one chemical core and, eventually, the Pd-catalyzed Suzuki-Miyaura cross-coupling led to the final set of selected items. The synthetic scheme adopted allowed us to easily obtain a library of molecules in view of future investigations of this promising core.

Biological evaluation through AlphaScreen assays led us to the identification of **14**, **16**, **18**, **22**, and **26** as new and selective agents, highlighting the 6-methylquinazolin-4(3H)-one as a valuable molecular platform for developing BRD9 binders. The here reported workflow highlights the possibility of investigating the quinazolin-4(3H)-one scaffold modulating further substitution patterns while guaranteeing the minimum requirements for BRD9 binding. This approach, based on coupling the advantages of *in silico* 3D structure-based pharmacophore-driven screening and of fast and efficient chemical synthesis procedures, can be re-iterated to produce different libraries of organic compounds in a rational and focused way as potential bioactive agents.

Experimental Section

Computational details

Docking calculation for 6-methylquinazolin-4(3H)-one scaffold

The 6-methylquinazolin-4(3H)-one scaffold was prepared using LigPrep software (Schrödinger Suite)^[15] accounting the protonation state at a pH = 7.4 ± 1.0 and minimizing the structure with OPLS 2005 force field. Prior to perform docking calculations, the Protein Preparation Wizard workflow (Maestro, Schrödinger) was employed using the crystal structure of the BRD9 bromodomain in complex

with BI-9564, the latter used as reference for grid box generation (PDB code:5F1H).^[10a] All hydrogen atoms were added, and bond orders were assigned. Docking calculations were performed using Glide software^[16] at standard precision (SP) level in order to perform an exhaustive sampling of all possible conformations in the BRD9 binding site.

Generation of the virtual library

Using CombiGlide software, a library of 673,680 6-methylquinazolin-4(3H)-one-based compounds was generated: 1203 aldehydes and 560 aromatic boronates were accounted according to the synthetic route (Scheme 2). For all generated compounds, the related pharmacokinetic properties were calculated using the Qikprop program in the Schrödinger Suite.^[17] After that, the new library was filtered using LigFilter, following the Lipinski filter to prioritize drug-like compounds and, finally, 174,992 compounds were selected for the subsequent molecular docking calculations.

Virtual screening of the generated library of 6-methylquinazolin-4(3H)-one derivatives

The generated library was used as input for molecular docking experiments, performed using the Virtual Screening Workflow tool as implemented in Schrödinger Suite and using Glide software^[16] considering three level of precision: High-Throughput Virtual Screening scoring and sampling (HTVS), Standard Precision scoring and sampling phase (SP), Extra Precision scoring and sampling phase (XP). Specifically, the following scheme was applied: after HTVS step, only 20% of the best poses were saved and used for the subsequent step; after SP level, only 20% of the best poses were saved and used for the subsequent step; in the XP level for each input were generated ten poses and finally 30% of the most promising items were saved for the final output. In addition, the free energy (ΔG_{bind}) was calculated for compounds 12–22 and 25–27 with the MM-GBSA method using the software Prime^[18] in the VSGB solvent model. The residues within 6 Å from the ligand were left free to move to reduce steric clashes (see Table S1).

Pharmacophore screening

The docking output contained 5267 poses, which were used as input for pharmacophore screening applying the developed 3D structure-based pharmacophore models (“pharm-druglike1” and “pharm-druglike2” 7-points models). Using the “Ligand and database screening” tool in Phase,^[19] for each compound the exact conformer arising from the molecular docking experiments, namely already accommodated in the chosen protein structure, was accounted through the “score in place” option. For the final selection, the output poses from the pharmacophore screening were further refined applying a cut-off of 2 kcal/mol from the best value of docking score and excluding poses featuring a PhaseScreen score < 1.25.

Molecular dynamics

The simulations of BRD9/22 and BRD9/23 complexes were carried out using the software Desmond^[20] with the OPLS-2005 force field. Initially, each complex was inserted in an orthorhombic box with a buffer distance of 10 Å in each space direction and solvated with TIP3P water molecules. The system charge was neutralized by adding Na⁺ or Cl⁻ ions. Subsequently, each system was relaxed following these steps: a Brownian Dynamics in NPT ensemble (i.e., keeping the number of molecules, the pressure, and the temper-

ature of the system constant) at 10 K for 100 ns, followed by two 12 ns steps at 10 K, in NVT and NPT ensemble respectively, with restrains on heavy solute atoms. Then, two phases of 12 ns and 24 ns, respectively, were carried out in an NPT ensemble at 300 K with and without restrains. After the relaxation phase, the systems were simulated for 100 ns in an NPT ensemble at 310 K.

Molecular dynamics analysis

Each trajectory was analyzed to extract qualitative information. In particular, the following properties were considered: a) the ligand root mean square deviation (RMSD) vs. the protein backbone, obtained measuring the RMSD of the ligand heavy atoms when the protein-ligand complex is first aligned on the protein backbone of the reference; b) the ligand RMSD vs. its reference conformation; c) protein-ligand contacts, monitoring the protein interactions during the simulations and categorizing them into six types: Hydrogen Bonds, Hydrophobic, Ionic and Water Bridges, π -cation and π - π stacking interactions.

Chemical synthesis

Chemistry general information

All commercially available starting materials were purchased from Merck Life Science srl and were used as received. The solvents used for the synthesis were of high-performance liquid chromatography (HPLC) grade (Merck Life Science S.R.L.). NMR spectra were recorded on a Bruker Avance 400 MHz instrument at T=298 K. All the compounds were dissolved in 0.5 mL of CDCl₃, CD₃OD or DMSO-d₆ (Merck Life Science S.R.L., 99.98 Atom % D). Coupling constants (*J*) are reported in Hertz, and chemical shifts are expressed in parts per million (ppm) on the delta (δ) scale relative to solvent peak as internal reference. Reactions were monitored on silica gel 60 F₂₅₄ plates (Merck Life Science S.R.L.) and visualized under UV light (λ = 254 nm, 365 nm). Analytical and semi-preparative reversed-phase HPLC was performed on Agilent Technologies 1200 Series high-performance liquid chromatography using a Fusion-RP, C reversed-phase column (100 × 2 mm, 4 μ m, 80 Å, flow rate = 1 mL/min; 250 × 10.00 mm, 4 μ m, 80 Å, flow rate = 4 mL/min respectively, Phenomenex). The binary solvent system (A/B) was as follows: 0.1% TFA in water (A) and 0.1% TFA in CH₃CN (B). The absorbance was detected at 250 nm. The purity of all tested compound (> 96%) were determined by NMR data.

Synthesis of compound 1

A solution of 2-amino-3-bromo-5-methylbenzoic acid (1.0 equiv), EDC HCl (1.5 equiv) and HOBT (1.65 equiv) in dry DCM/DMF(10/1, 100 ml) was treated with DIPEA (6.5 equiv). The resulting mixture was stirred for 5 hours at room temperature under N₂ atmosphere. After that NH₄Cl was added (3.25 equiv), the reaction continued for 20 h in the same conditions. The organic layer was washed with HCl 1 N (3 × 15 ml), dried over Na₂SO₄ and concentrated to obtain the final products. The crude was pure to use for the next step without any purification.

General procedure a for the synthesis of intermediates 2–10

A solution of 2-amino-3-bromo-5-methylbenzamide (1) (1.0 equiv) and selected benzaldehyde (1.2 equiv) in dry THF (30 mL) was stirred for 5 h at reflux; then, molecular I₂ (5.0 equiv) was added. The reaction was stirred over-night at reflux. Then, the mixture was diluted with DCM (20 mL) and washed with a water solution of

thiosulfate (2×10 mL) and brine (2×10 mL), dried over anhydrous Na₂SO₄, filtered, and concentrated *in vacuo*. The desired compounds were purified by silica gel using different mixtures of hexane/acetate depending on the polarity of the molecule.

General procedure b for the synthesis of intermediate 11

To a solution of 2-amino-3-bromo-5-methylbenzamide (1) (1.0 equiv) in EtOH, tert-butyl hydroperoxide (3.8 equiv) was added. The mixture was stirred overnight at reflux. After the completion of the reaction, the mixture was concentrated, diluted with CHCl₃ and washed three times (3×10 mL). The organic layer was dried over anhydrous Na₂SO₄, filtered and concentrated under reduced pressure to afford the crude product. The final product was obtained by silica gel purification using a mixture of hexane/ethyl acetate (65/35 v/v).

General procedure c for the synthesis of compounds 12–27

8-bromo-6-methylquinazolin-4(3H)-one (1.0 equiv), the selected boronic acid (1.5 equiv), K₂CO₃ (3.0 equiv) and tetrakis(triphenylphosphine)palladium(0) (0.2 equiv) were dissolved in a previously degassed mixture of 1,4-dioxane (80%) and water (20%) (20 mL) and stirred over-night at 80 °C under argon atmosphere. After the completion of the reaction, the mixture was diluted with DCM and washed with brine (3×10 mL). The organic layer was dried over anhydrous Na₂SO₄, filtered, and concentrated under reduced pressure to afford the crude product. The resulting residue was purified on a silica gel column chromatography eluting with different hexane/ethyl acetate mixtures to give the final products.

In vitro Alpha Screen assay

The binding of synthesized compounds against BRD9 and BRD4 BD1 was measured by Alpha Screen Technology through BRD9 (BD1) Inhibitor Screening Assay Kit (BSP-32519) and BRD4 (BD1) Inhibitor Screening Assay Kit (BSP-32514). Anti-GST-coated acceptor beads were used to capture the GST-fusion BRD9, whereas the biotinylated-H4 peptide (BET bromodomain ligand) was captured by the streptavidin donor beads. Upon illumination at 680 nm, chemical energy is transferred from donor to acceptor beads across the complex streptavidin-donor/H4-biotin/GST-BRD/anti-GST-acceptor and a signal is produced. The assay was performed in white, 384-well Optiplates (Perkin Elmer) using a final volume of 30 μL containing final concentrations of 50 nM of purified GST-tagged BRD protein (BSP-31091 and BSP-31040), 1 μL of BET bromodomain ligand (BSP-33000). 10 μL of 250-fold diluted Glutathione AlphaLISA Acceptor Beads (PerkinElmer #AL109 C) and 10 μL of 150-fold diluted Streptavidin Donor Bead (PerkinElmer #6760002) were used for BRD9 screening assay. Instead, 10 μL of 250-fold diluted Glutathione AlphaLISA Acceptor Beads (PerkinElmer #AL109 C) and 10 μL of 250-fold diluted Streptavidin Donor Bead (PerkinElmer #6760002) were used for BRD4 screening assay. The concentration of DMSO was maintained at a final concentration of 0.5% in each well. The stimulation times with 10 μL of tested compound (each at final concentration of 10 μM) were fixed to 30 min at room temperature. After the addition of the detection acceptor beads, the plates were incubated in the dark for 30 min at room temperature and finally read in an Enspire microplate analyzer (Perkin Elmer).

Acknowledgements

The research leading to these results has received funding from AIRC under MFAG 2017-ID. 20160 project- P.I. Lauro Gianluigi. Open Access funding provided by Università degli Studi di Salerno within the CRUI-CARE Agreement.

Conflict of Interest

The authors declare no conflict of interest.

Data Availability Statement

The data that support the findings of this study are available from the corresponding author upon reasonable request.

Keywords: Antitumor agents · Combinatorial chemistry · Cyclization · Drug design · Structure-activity relationships

- [1] P. Filippakopoulos, S. Picaud, M. Mangos, T. Keates, J.-P. Lambert, D. Barsyte-Lovejoy, I. Felletar, R. Volkmer, S. Müller, T. Pawson, A.-C. Gingras, C. H. Arrowsmith, S. Knapp, *Cell* **2012**, *149*, 214–231.
- [2] Y. Taniguchi, *Int. J. Mol. Sci.* **2016**, *17*, 1849–1873.
- [3] a) X. Zhu, Y. Liao, L. Tang, *OncoTargets Ther.* **2020**, *13*, 13191–13200; b) G. M. Euskirchen, R. K. Auerbach, E. Davidov, T. A. Gianoulis, G. Zhong, J. Rozowsky, N. Bhardwaj, M. B. Gerstein, M. Snyder, *PLoS Genet.* **2011**, *7*, e1002008.
- [4] M. Hui, Z. Jian, Z. Peiyuan, W. Zhenwei, Z. Huibin, *Future Med. Chem.* **2018**, *10*, 895–906.
- [5] a) S. Gatadi, T. V. Lakshmi, S. Nanduri, *Eur. J. Med. Chem.* **2019**, *170*, 157–172; b) M. S. Malamas, J. Millen, *J. Med. Chem.* **1991**, *34*, 1492–1503; c) J. F. Wolfe, T. L. Rathman, M. C. Sleevi, J. A. Campbell, T. D. Greenwood, *J. Med. Chem.* **1990**, *33*, 161–166; d) S. Liu, D. Yuan, S. Li, R. Xie, Y. Kong, X. Zhu, *Eur. J. Med. Chem.* **2021**, *225*, 113764.
- [6] M. Pierrì, E. Gazzillo, M. G. Chini, M. G. Ferraro, M. Piccolo, F. Maione, C. Irace, G. Bifulco, I. Bruno, S. Terracciano, G. Lauro, *Bioorg. Chem.* **2022**, *118*, 105480.
- [7] B. A. Bhat, D. P. Sahu, *Synth. Commun.* **2004**, *34*, 2169–2176.
- [8] X. Chang, D. Sun, D. Shi, G. Wang, Y. Chen, K. Zhang, H. Tan, J. Liu, B. Liu, L. Ouyang, *Acta Pharma. Sin.* **2021**, *11*, 156–180.
- [9] M. Bhat, S. L. Belagali, S. V. Mamatha, B. K. Sagar, E. V. Sekhar, *Stud. Nat. Prod. Chem.* **2021**, *71*, 185–219.
- [10] a) L. J. Martin, M. Koegl, G. Bader, X.-L. Cockcroft, O. Fedorov, D. Fiegen, T. Gerstberger, M. H. Hofmann, A. F. Hohmann, D. Kessler, S. Knapp, P. Knesl, S. Kornigg, S. Müller, H. Nar, C. Rogers, K. Rumpel, O. Schaaf, S. Steurer, C. Tallant, C. R. Vakoc, M. Zeeb, A. Zoephel, M. Pearson, G. Boehmelt, D. McConnell, *J. Med. Chem.* **2016**, *59*, 4462–4475; b) S. Picaud, M. Strocchia, S. Terracciano, G. Lauro, J. Mendez, D. L. Daniels, R. Riccio, G. Bifulco, I. Bruno, P. Filippakopoulos, *J. Med. Chem.* **2015**, *58*, 2718–2736; c) N. H. Theodoulou, P. Bamborough, A. J. Bannister, I. Becher, R. A. Bit, K. H. Che, C.-W. Chung, A. Dittmann, G. Drewes, D. H. Drewry, L. Gordon, P. Grandi, M. Leveridge, M. Lindon, A.-M. Michon, J. Molnar, S. C. Robson, N. C. O. Tomkinson, T. Kouzarides, R. K. Prinjha, P. G. Humphreys, *J. Med. Chem.* **2015**, *59*, 1425–1439; d) P. G. Clark, L. C. Vieira, C. Tallant, O. Fedorov, D. C. Singleton, C. M. Rogers, O. P. Monteiro, J. M. Bennett, R. Baronio, S. Müller, D. L. Daniels, J. Méndez, S. Knapp, P. E. Brennan, D. J. Dixon, *Angew. Chem. Int. Ed. Engl.* **2015**, *54*, 6217–6221.
- [11] M. G. Chini, G. Lauro, G. Bifulco, *Eur. J. Org. Chem.* **2021**, *2021*, 2966–2981.
- [12] a) C. Larksarp, H. Alper, *J. Org. Chem.* **2000**, *65*, 2773–2777; b) H. Li, L. He, H. Neumann, M. Beller, X.-F. Wu, *Green Chem.* **2014**, *16*, 1336–1343; c) P. Salehi, M. Dabiri, M. A. Zolfigol, M. Baghbanzadeh, *Tetrahedron Lett.* **2005**, *46*, 7051–7053.

- [13] R. M. Eglén, T. Reisine, P. Roby, N. Rouleau, C. Illy, R. Bossé, M. Bielefeld, *Curr. Chem. Genomics* **2008**, *1*, 2–10.
- [14] a) J. Su, X. Liu, S. Zhang, F. Yan, Q. Zhang, J. Chen, *Chem. Biol. Drug Des.* **2019**, *93*, 163–176; b) S. De Vita, M. G. Chini, G. Bifulco, G. Lauro, *Molecules* **2021**, *26*, 7192.
- [15] *Schrödinger Release 2021–1: LigPrep*, Schrödinger LLC, New York, NY, **2021**.
- [16] a) R. A. Friesner, J. L. Banks, R. B. Murphy, T. A. Halgren, J. J. Klicic, D. T. Mainz, M. P. Repasky, E. H. Knoll, M. Shelley, J. K. Perry, *J. Med. Chem.* **2004**, *47*, 1739–1749; b) R. A. Friesner, R. B. Murphy, M. P. Repasky, L. L. Frye, J. R. Greenwood, T. A. Halgren, P. C. Sanschagrin, D. T. Mainz, *J. Med. Chem.* **2006**, *49*, 6177–6196; c) T. A. Halgren, R. B. Murphy, R. A. Friesner, H. S. Beard, L. L. Frye, W. T. Pollard, J. L. Banks, *J. Med. Chem.* **2004**, *47*, 1750–1759; d) *Schrödinger Release 2021–1: Glide*, Schrödinger LLC, New York, NY, **2021**.
- [17] a) *Schrödinger Release 2021–1: QikProp*, Schrödinger LLC, New York, NY, **2021**; b) A. Laoui, V. R. Polyakov, *J. Comput. Chem.* **2011**, *32*, 1944–1951.
- [18] a) M. P. Jacobson, D. L. Pincus, C. S. Rapp, T. J. F. Day, B. Honig, D. E. Shaw, R. A. Friesner, *Proteins Struct. Funct. Genet.* **2004**, *55*, 351–367; b) M. P. Jacobson, R. A. Friesner, Z. Xiang, B. Honig, *J. Mol. Biol.* **2002**, *320*, 597–608; c) *Schrödinger Release 2021–1: Prime*, Schrödinger LLC, New York, NY, **2021**.
- [19] a) *Schrödinger Release 2021–1: Phase*, Schrödinger LLC, New York, NY, **2021**; b) S. L. Dixon, A. M. Smondyrev, E. H. Knoll, S. N. Rao, D. E. Shaw, R. A. Friesner, *J. Comput.-Aided Mol. Des.* **2006**, *20*, 647–671; c) S. L. Dixon, A. M. Smondyrev, S. N. Rao, *Chem. Biol. Drug Des.* **2006**, *67*, 370–372.
- [20] a) *Schrödinger Release 2021–1: Desmond*, Schrödinger LLC, New York, NY, **2021**. Desmond Molecular Dynamics System, D. E. Shaw Research, New York, NY, **2021**. Maestro-Desmond Interoperability Tools, Schrödinger LLC, New York, NY, **2021**; b) K. J. Bowers, D. E. Chow, H. Xu, R. O. Dror, M. P. Eastwood, B. A. Gregersen, J. L. Klepeis, I. Kolossvary, M. A. Moraes, F. D. Sacerdoti, J. K. Salmon, Y. Shan, D. E. Shaw in *SC '06: Proceedings of the 2006 ACM/IEEE Conference on Supercomputing, Tampa, FL, USA, 11–17 November 2006*, Association for Computing Machinery, New York, NY, USA, **2006**; pp. 43.
- [21] S. Parua, S. Das, R. Sikari, S. Sinha, N. D. Paul, *J. Org. Chem.* **2017**, *82*, 7165–7175.

Manuscript received: July 19, 2022
Revised manuscript received: August 4, 2022
Accepted manuscript online: August 5, 2022